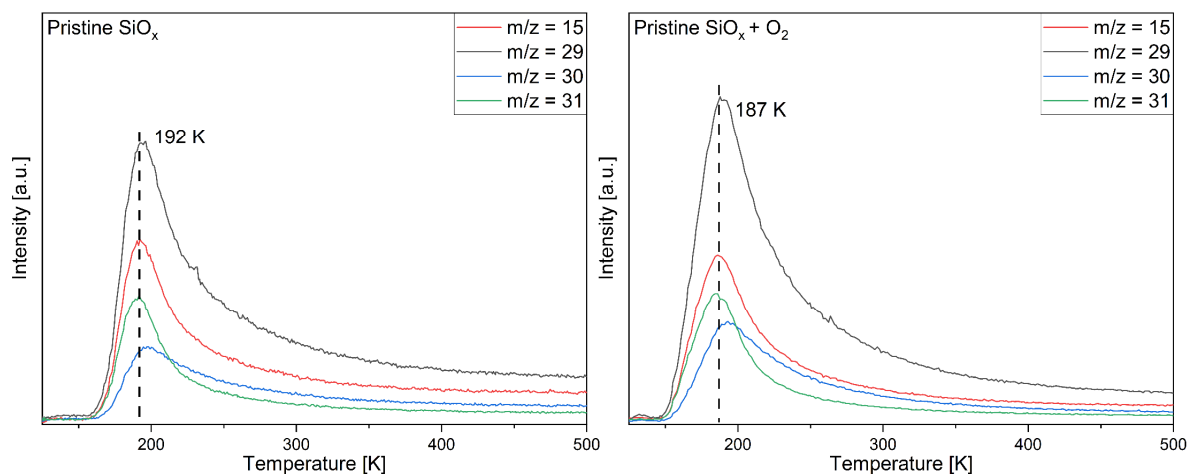
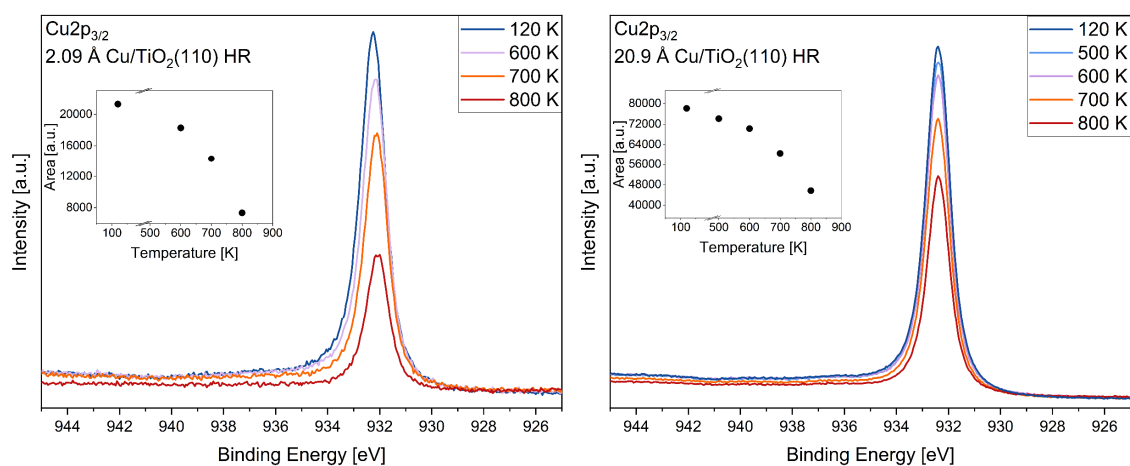


## SUPPLEMENTARY INFORMATION



**Figure S1:** TPR spectra of a monolayer methanol (left spectrum) adsorbed at  $T = 115$  K and methanol adsorbed with 75 L of oxygen pre-adsorbed (right spectrum) at the cleaned pristine silicon wafer. Only signals were visible that corresponded to the molecular desorption of methanol. Other masses that correspond to methanol are not shown for clarity. The sample was heated with  $2 \text{ K s}^{-1}$ .



**Figure S2:** Temperature-dependent X-ray photoelectron Cu<sub>2p<sub>3/2</sub></sub> spectra of a) 2.09 Å and b) 20.9 Å of copper deposited onto highly reduced TiO<sub>2</sub>(110). The pristine spectra were measured at  $T = 120$  K. Then, the samples were heated to the specific temperature and held there for 10 minutes. XP-spectra were taken after cooling down to 120 K again.

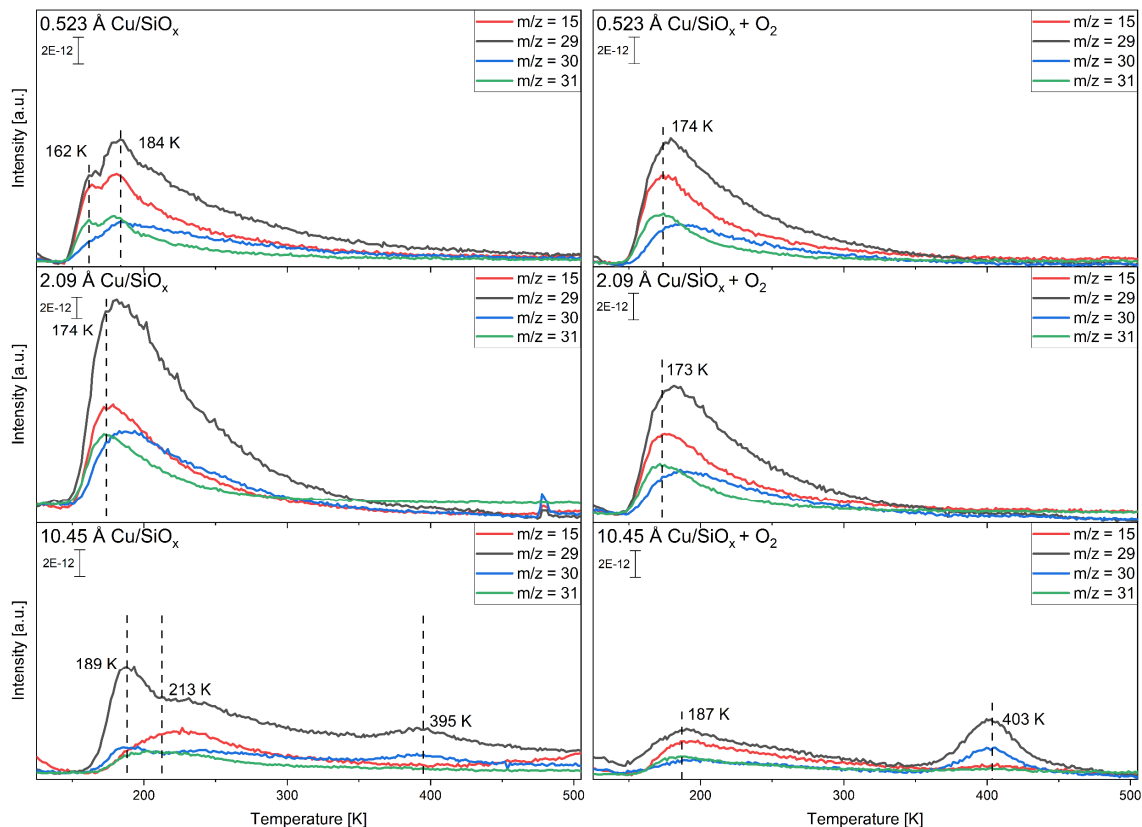


**Fig S3:** Copper coverage dependent TPR spectra of a monolayer methanol (left spectra) adsorbed at  $T = 115$  K and methanol adsorbed with 75 L of oxygen pre-adsorbed (right spectra) at copper deposited onto  $\text{SiO}_x$ . Shown are the relevant  $m/z$  for methanol ( $m/z = 31$ ), formaldehyde ( $m/z = 29, 30$ ), and methane ( $m/z = 15$ ), as well as the contribution from the carbon monoxide isotope desorption ( $m/z = 29, 30$ ). The samples were heated with  $2 \text{ K s}^{-1}$ .

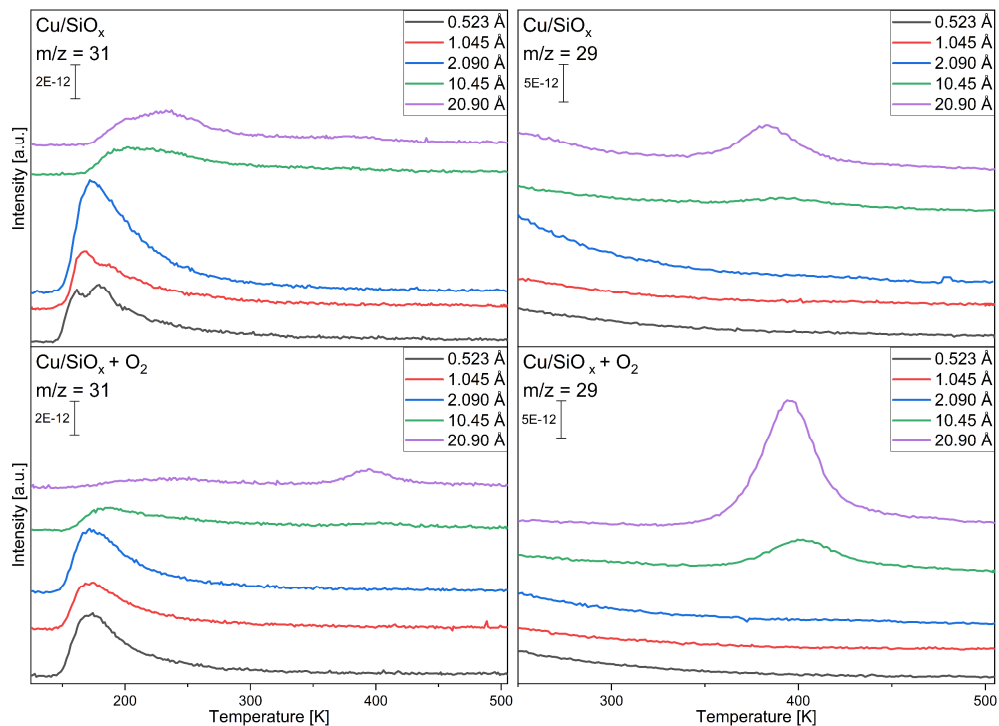


**Figure S4:** Copper coverage-dependent TPR spectra of a monolayer methanol (top spectra) adsorbed at  $T = 115$  K and methanol with 75 L of oxygen pre-adsorbed (bottom spectra) at copper deposited onto  $\text{SiO}_x$ . Presented are the evolution of the  $m/z = 31$  for methanol (left spectra) and the  $m/z = 29$  for formaldehyde (right spectra). The samples were heated with  $2 \text{ K s}^{-1}$ .

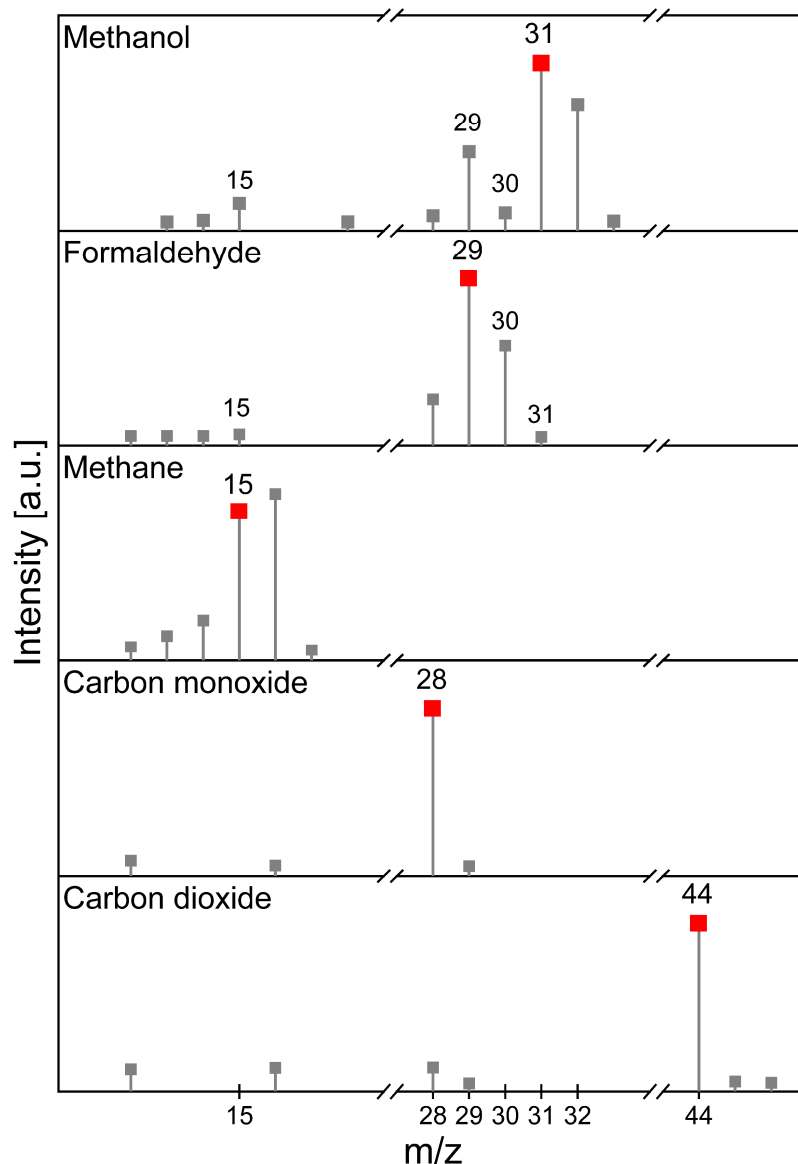


**Figure S5:** Fragmentation pattern of methanol and selected observed possible products. The fragmentation patterns were taken from the NIST Database<sup>1</sup> for electron ionization mass spectra. Marked in red are the selected mass-to-charge ratios used to identify the specific products. It must be noted that the actual fragmentation can differ from the presented data due to the specification of the used quadrupole mass spectrometer.

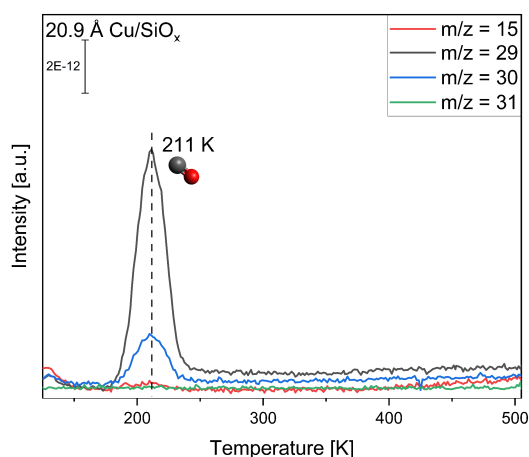


**Figure S6:** TPR spectrum of the blank silicon wafer with 20.9 Å of copper deposited onto the surface. Only a rise in  $m/z = 29$  and  $m/z = 30$  is visible which corresponds most likely to carbon monoxide isotope signals as  $m/z = 28$  is also visible rising at the same time (not shown). This carbon monoxide contamination may be attributed to the chamber background. Carbon monoxide was found to desorb at different temperatures, depending on the saturation coverage. Carbon monoxide first adsorbs at step edges, desorbing at around 210 K and afterward on terraces, desorbing at 170 K and 138 K for various copper single crystal surfaces from Cu(110), Cu(110), Cu(311) and Cu(410).<sup>2-5</sup> The 211 K desorption from the copper-covered substrates would suggest that carbon monoxide binds on the step edges of the rough copper clusters.

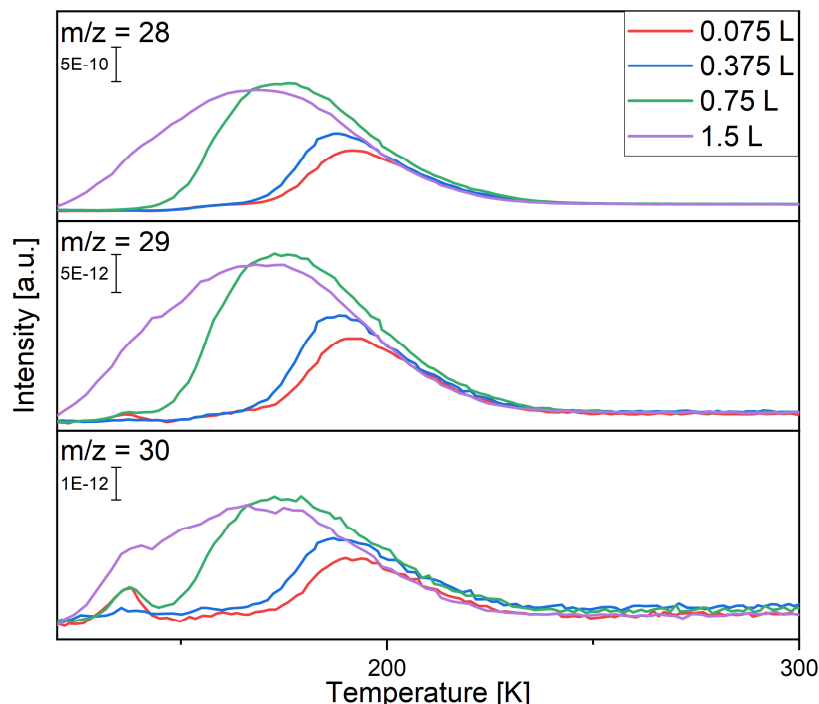


**Figure S7:** TPR spectra of carbon monoxide adsorbed at  $T = 115$  K at 10.45 Å of Cu deposited onto slightly reduced  $\text{TiO}_2(110)$ . The carbon monoxide (Air liquid, 99.997 %) was adsorbed onto the surface via backfilling of the UHV-chamber between  $10^{-9}$  and  $10^{-8}$  mbar resulting in a theoretical coverage between 0.075 L and 1.5 L. Shown are the  $m/z = 29$  (top) and  $m/z = 28$  (middle) and  $m/z = 30$  (bottom). Depending on the coverage three different species at 191 K, 174 K, and 137 K are apparent. All three desorption species are in good accordance with data from copper single crystals.<sup>2-5</sup> The similar shape and coherent intensities confirm that the

signals in the  $m/z = 29$  and  $m/z = 30$  relate to carbon monoxide isotopes desorbing from the surface.<sup>6</sup> We must note that the desorption at 137 K could be influenced by desorption from the filament and other sample holder parts when starting the heat ramp as seen especially in the  $m/z = 30$ .

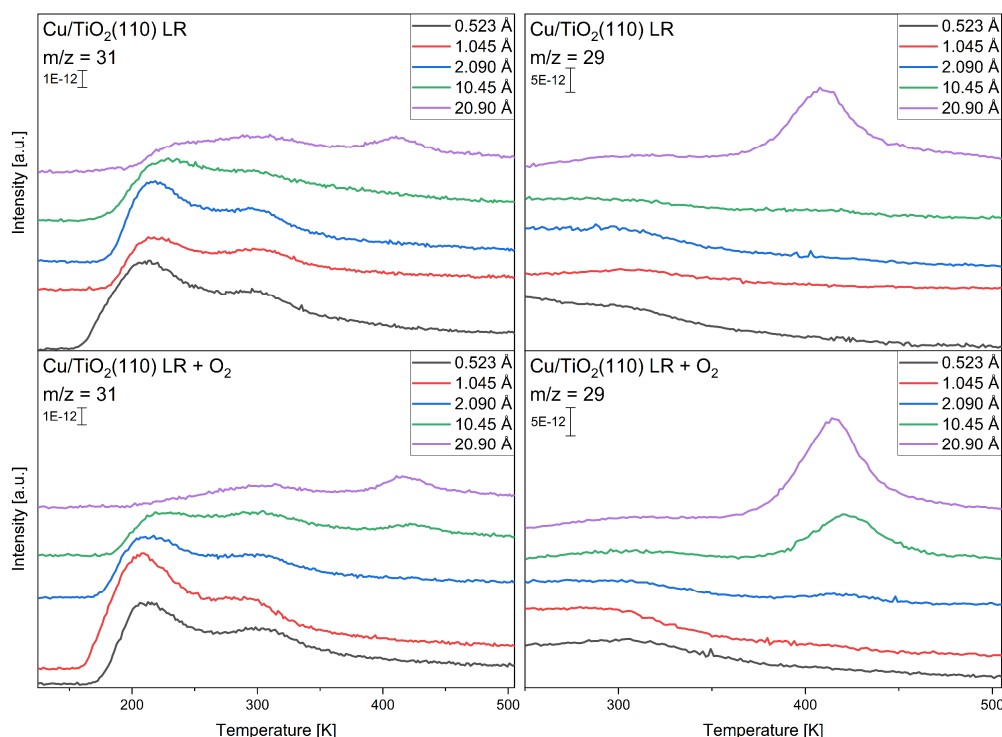


**Figure S8:** Copper coverage-dependent TPR spectra of a monolayer methanol (top spectra) adsorbed at  $T = 115$  K and methanol with 75 L of oxygen pre-adsorbed (bottom spectra) at copper deposited onto the slightly reduced  $\text{TiO}_2(110)$  crystal. Presented is the evolution of the  $m/z = 31$  for methanol (left spectra) and the  $m/z = 29$  for formaldehyde (right spectra). The samples were heated with  $2 \text{ K s}^{-1}$ .

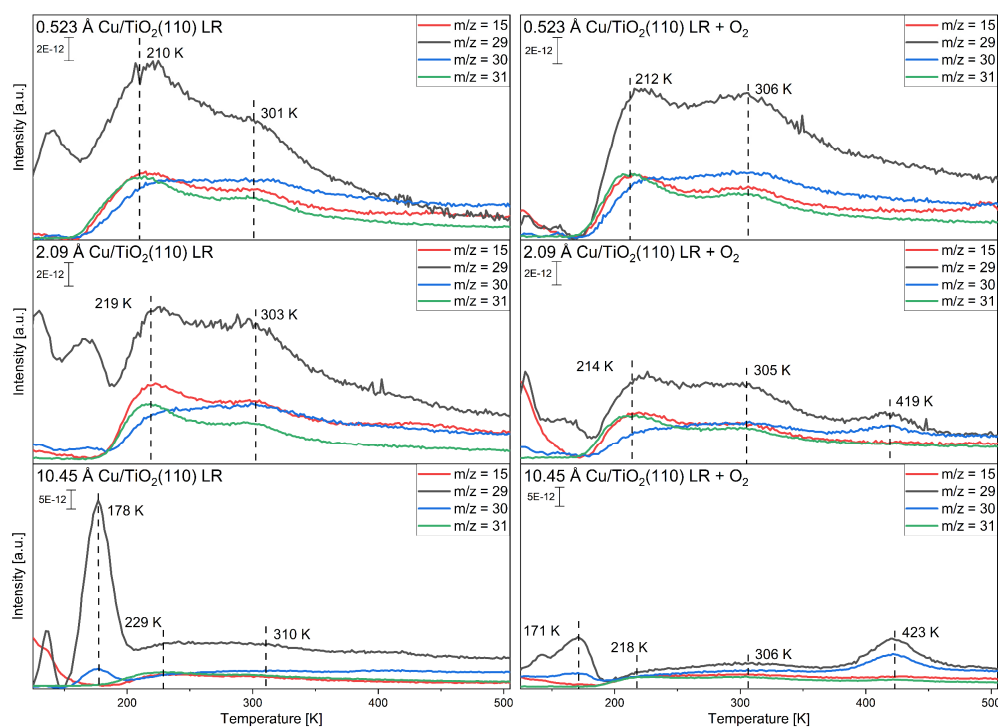


**Figure S9:** Copper coverage-dependent TPR spectra of a monolayer methanol adsorbed (left spectra) at  $T = 115$  K and methanol with 75 L of oxygen pre-adsorbed (right spectra) at copper

deposited onto the slightly reduced  $\text{TiO}_2(110)$  crystal. Shown are the relevant  $m/z$  for methanol ( $m/z = 31$ ), formaldehyde ( $m/z = 29, 30$ ), and methane ( $m/z = 15$ ), as well as the contribution from the carbon monoxide isotope desorption ( $m/z = 29,30$ ). The samples were heated with  $2 \text{ K s}^{-1}$ .

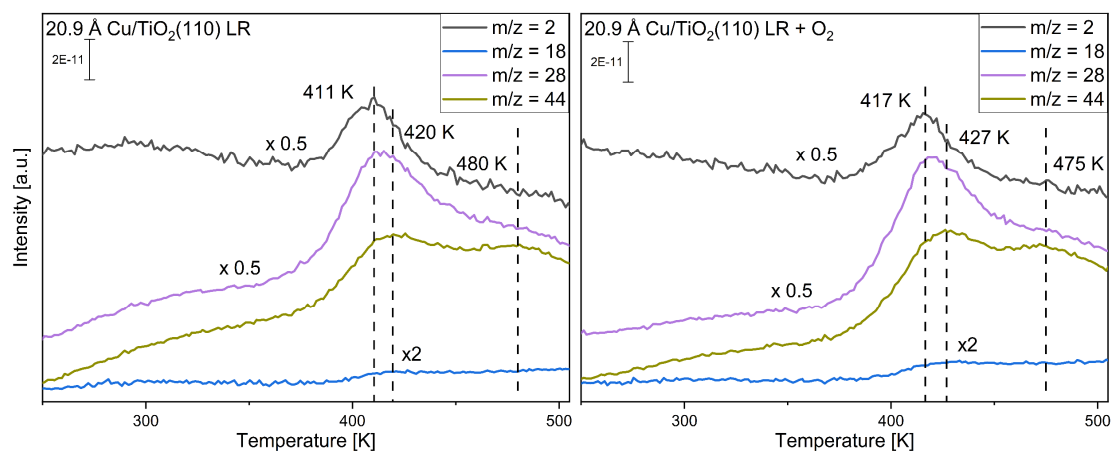


**Figure S10:** TPR spectra of a monolayer methanol (left spectrum) adsorbed at  $T = 115 \text{ K}$  and methanol with  $75 \text{ L}$  of oxygen pre-adsorbed (right spectrum) at  $20.9 \text{ Å}$  of copper deposited onto the slightly reduced  $\text{TiO}_2(110)$  crystal. Shown are the responsive  $m/z$  for hydrogen ( $m/z = 2$ ), carbon monoxide ( $m/z = 28$ ), carbon dioxide ( $m/z = 44$ ) and water ( $m/z = 18$ ). For better visibility, the signal of  $m/z = 2$  and  $m/z = 28$  were divided by two and the signal of  $m/z = 18$  was multiplied by two. The sample was heated with  $2 \text{ K s}^{-1}$ .

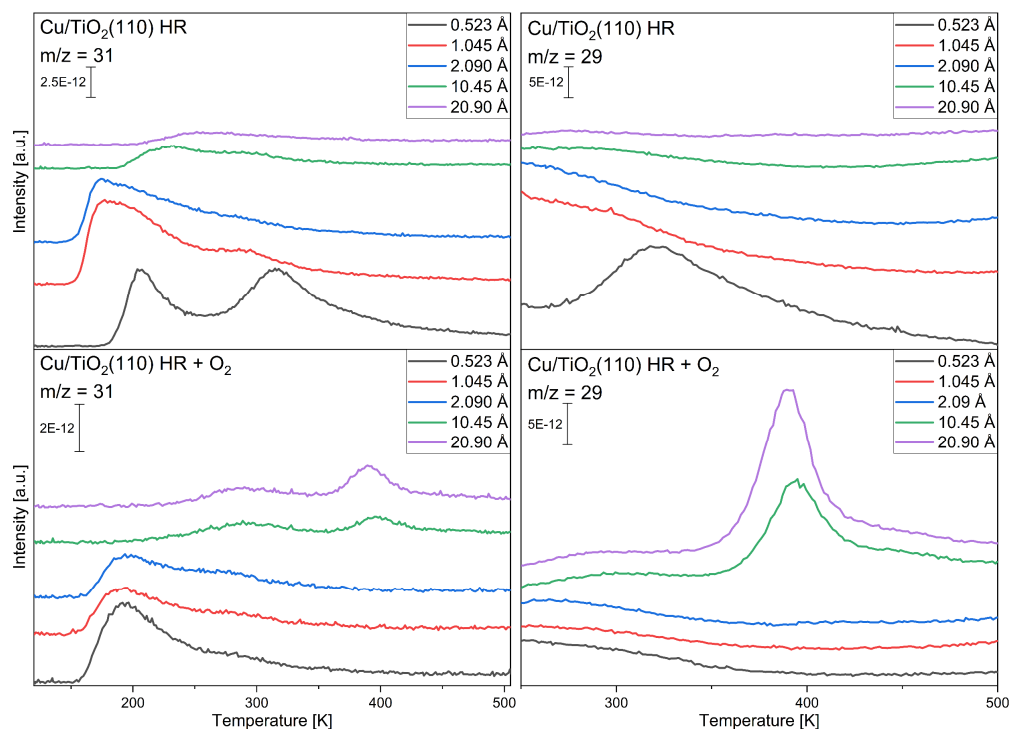


**Figure S11:** Copper coverage-dependent TPR spectra of a monolayer methanol (top spectra) adsorbed at  $T = 115 \text{ K}$  and methanol with  $75 \text{ L}$  of oxygen pre-adsorbed (bottom spectra) at copper deposited onto the highly reduced  $\text{TiO}_2(110)$  crystal. Presented is the evolution of the  $m/z = 31$  for methanol (left spectra) and the  $m/z = 29$  for formaldehyde (right spectra). The samples were heated with  $2 \text{ K s}^{-1}$ .

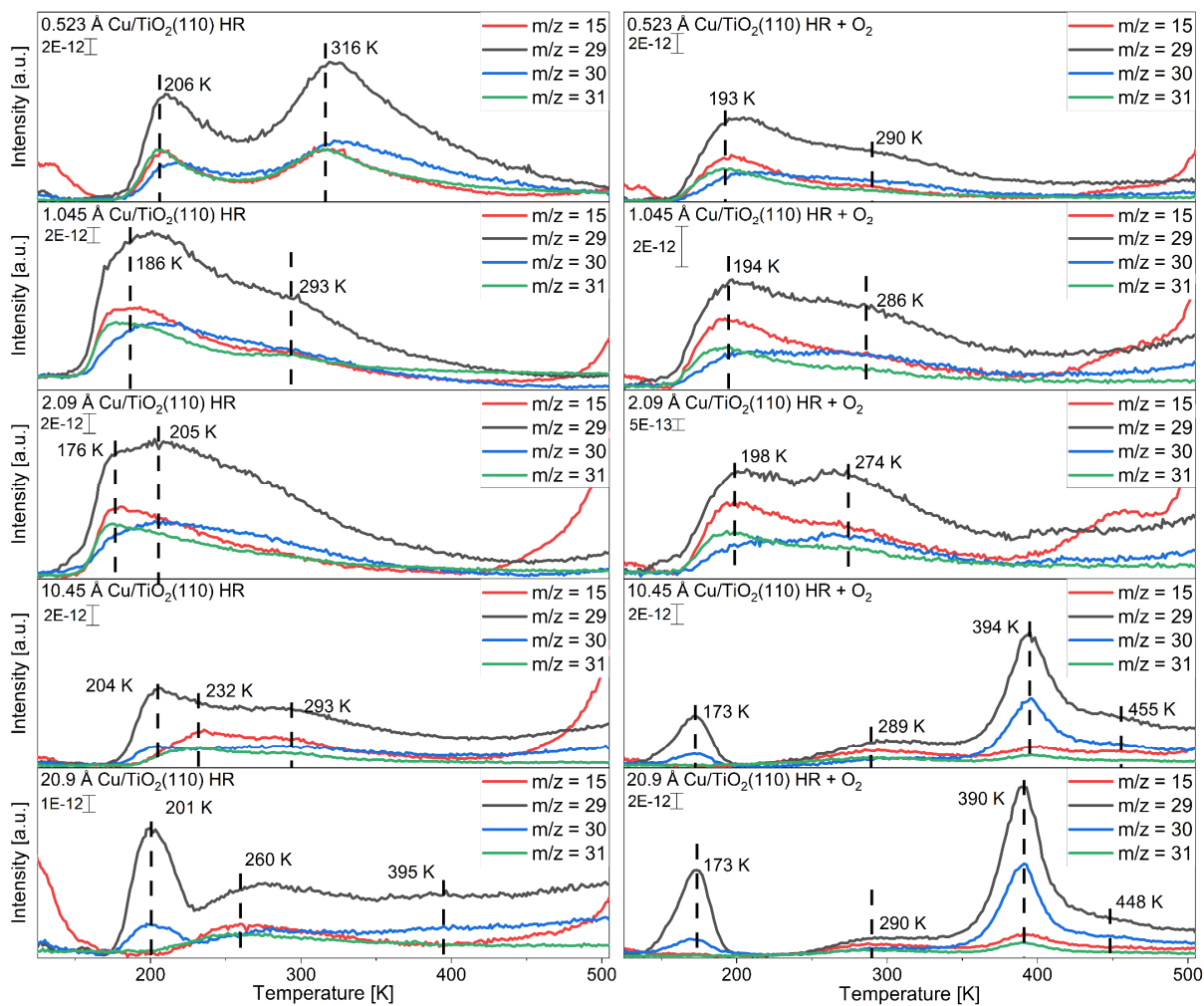


**Figure S12:** Copper coverage-dependent TPR spectra of a monolayer methanol (left spectra) adsorbed at  $T = 115$  K and methanol with 75 L of oxygen pre-adsorbed (right spectra) with copper deposited onto the highly reduced  $\text{TiO}_2(110)$  crystal. Shown are the relevant  $m/z$  for methanol ( $m/z = 31$ ), formaldehyde ( $m/z = 29, 30$ ), and methane ( $m/z = 15$ ), as well as the contribution from the carbon monoxide isotope desorption ( $m/z = 29, 30$ ). The samples were heated with  $2 \text{ K s}^{-1}$ .



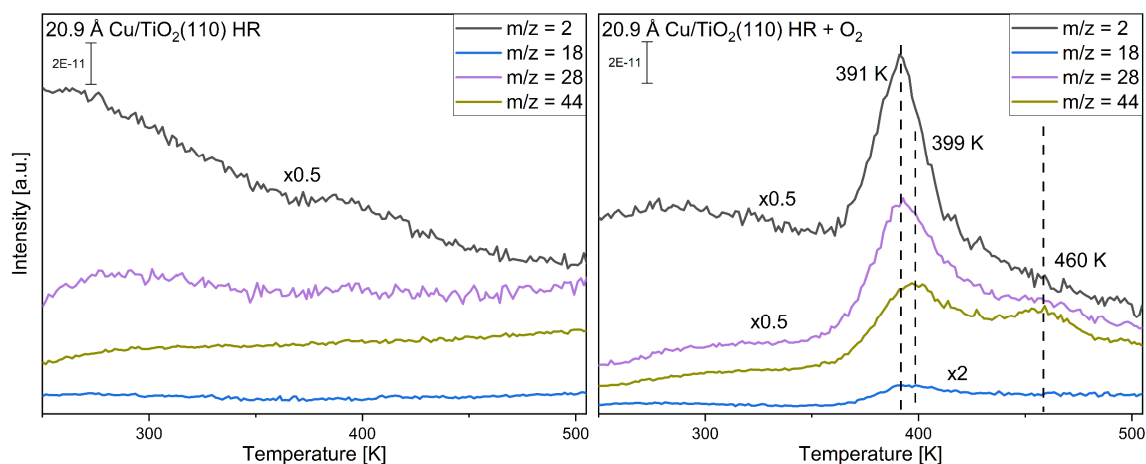


**Figure S13:** TPR spectra of a monolayer methanol (left spectrum) adsorbed at  $T = 115$  K and methanol with 75 L of oxygen pre-adsorbed (right spectrum) with 20.9 Å of copper deposited onto the highly reduced  $\text{TiO}_2(110)$  crystal. Shown are the responsive  $m/z$  for hydrogen ( $m/z = 2$ ), carbon monoxide ( $m/z = 28$ ), carbon dioxide ( $m/z = 44$ ) and water ( $m/z = 18$ ). For better visibility, the signal of  $m/z = 2$  and  $m/z = 28$  were divided by two and the signal of  $m/z = 18$  was multiplied by two. The sample was heated with  $2 \text{ K s}^{-1}$ .

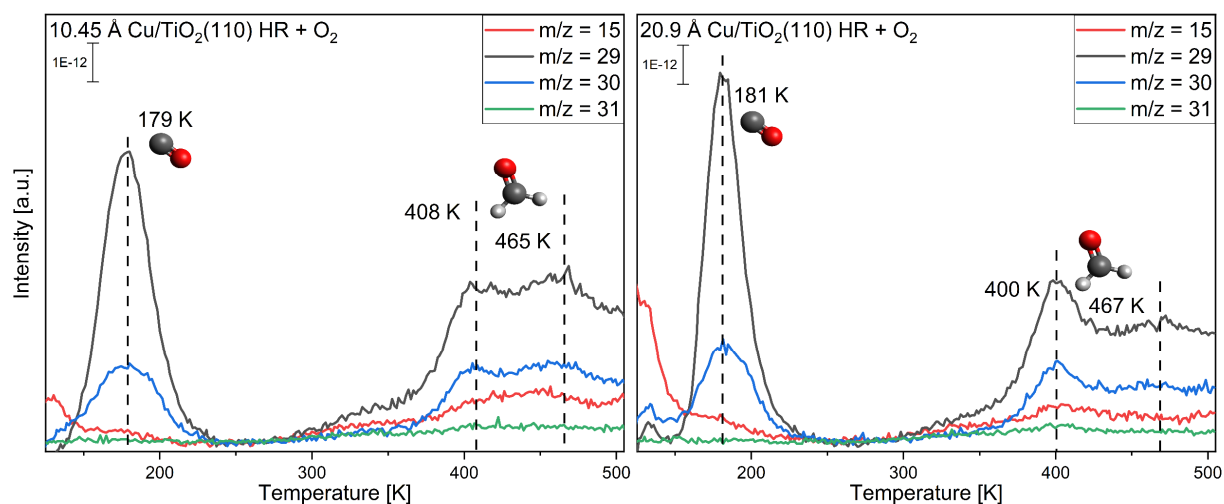


**Figure S14:** TPR spectra of a sub-monolayer methanol adsorbed at  $T = 115$  K with 75 L of oxygen co-adsorbed at the highly reduced  $\text{TiO}_2(110)$  crystal for 10.45 Å Cu and 20.9 Å Cu. Shown are the relevant  $m/z$  for methanol ( $m/z = 31$ ), formaldehyde ( $m/z = 29, 30$ ), and methane ( $m/z = 15$  as well as some contribution from the carbon monoxide isotope desorption ( $m/z = 29, 30$ )). The samples were heated with  $2 \text{ K s}^{-1}$ .

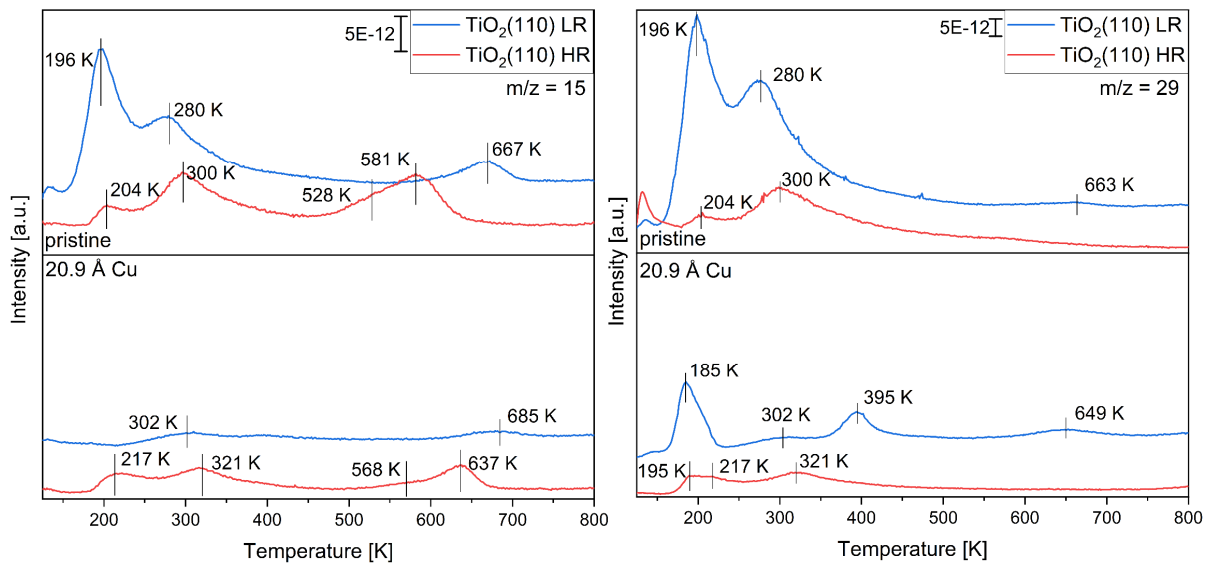


**Figure S15:** TPR spectra of a monolayer methanol adsorbed at  $T = 115$  K at the pristine slightly (LR) and highly (HR) reduced  $\text{TiO}_2(110)$  single crystals and 20.9 Å of copper deposited onto the slightly and highly reduced single crystals. Presented are the  $m/z = 15$  and  $m/z = 29$  for the experiments to 800 K with an increase in temperature by  $2 \text{ K s}^{-1}$ .

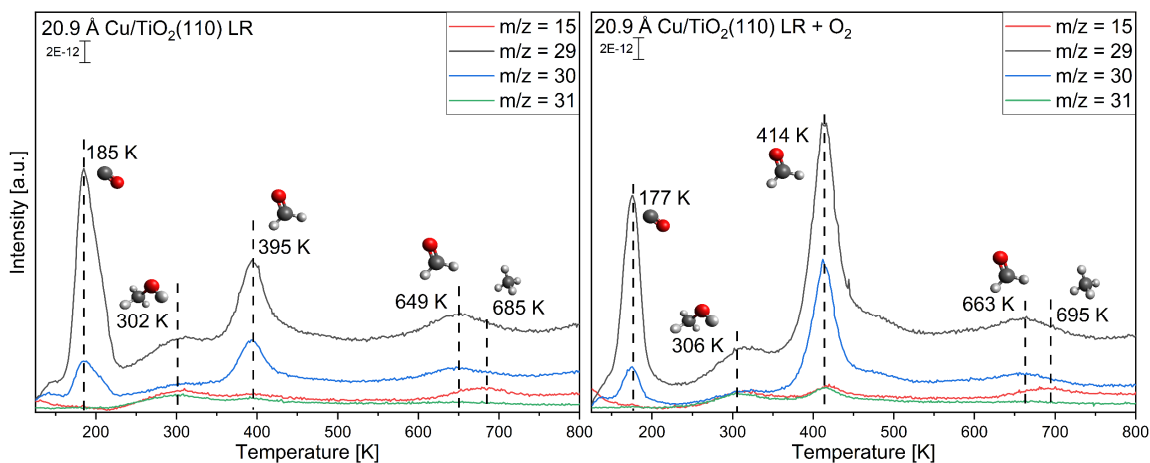


**Figure S16:** TPR spectra of a monolayer methanol (left spectrum) adsorbed at  $T = 115$  K and methanol with 75 L of oxygen pre-adsorbed (right spectrum) at 20.9 Å of copper deposited at the slightly reduced  $\text{TiO}_2(110)$  crystal. Shown are the relevant  $m/z$  for methanol ( $m/z = 31$ ), formaldehyde ( $m/z = 29, 30$ ), and methane ( $m/z = 15$ ), as well as the contribution from the carbon monoxide isotope desorption ( $m/z = 29, 30$ ). In comparison to earlier TPRS experiments, the sample was heated to 800 K with  $2 \text{ K s}^{-1}$  within the experiments. The spectrum with oxygen pre-adsorption was taken directly after the experiments to 500 K, while the spectrum without oxygen was measured afterward. Since heating over 500 K influences the properties of the copper clusters, a difference in comparison to Fig 4 cannot be neglected. Even then, the formaldehyde formation from copper (395 K and 414 K) is still overwhelming the formaldehyde formation on  $\text{TiO}_2$  (649 K and 663 K) and the methane formation on  $\text{TiO}_2$  (685 K and 695 K).

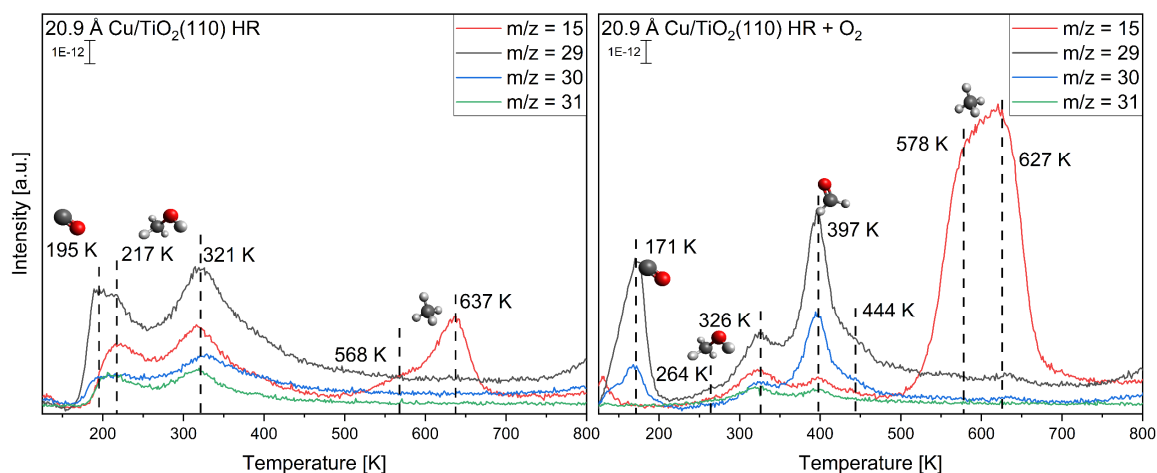


**Figure S17:** TPR spectra of a monolayer methanol (left spectrum) adsorbed at  $T = 115$  K and methanol with 75 L of oxygen pre-adsorbed (right spectrum) at 20.9 Å of copper deposited onto the slightly reduced  $\text{TiO}_2(110)$  crystal. Shown are the relevant  $m/z$  for methanol ( $m/z = 31$ ), formaldehyde ( $m/z = 29, 30$ ), and methane ( $m/z = 15$ ), as well as the contribution from the carbon monoxide isotope desorption ( $m/z = 29, 30$ ). In comparison to earlier TPRS experiments, the sample was heated to 800 K with  $2 \text{ K s}^{-1}$ . Since heating over 500 K influences the properties of the copper clusters, a difference in comparison to Fig S12 cannot be neglected. The same desorption signals were apparent as in Fig S12, with only methane forming at temperatures above 500 K.

**Table S1:** Temperature programmed X-ray photoelectron spectroscopy parameters for the experiment of copper deposited onto  $\text{SiO}_x$ .

Spectrum	Pass energy [eV]	Energy step size [eV]	Dwell time [ms]	Loops	Interval [eV] (BE)	Temperature ramp [ $\text{K s}^{-1}$ ]
$\text{Cu}2p_{3/2}$	30	0.15	25	90	928 – 938	0.5

**Table S2:** X-ray photoelectron spectroscopy parameters for the temperature experiments of copper on the slightly reduced  $\text{TiO}_2(110)$  single crystal.

Spectrum	Pass energy [eV]	Energy step size [eV]	Dwell time [ms]	Number of scans	Interval [eV] (BE)
$\text{Cu}2p_{3/2}$	20	0.05	100	10	925 – 950

- 1 NIST Mass Spectrometry Data Center, NIST Standard Reference Database Number 69: NIST Chemistry WebBook, <https://webbook.nist.gov/>, (accessed 15 July 2024).
- 2 T. Makino and M. Okada, *Surf. Sci.*, 2014, **628**, 36–40.
- 3 A. Kokalj, T. Makino and M. Okada, *J. Phys. Condens. Matter*, 2017, **29**, 194001.
- 4 T. Sueyoshi, T. Sasaki and Y. Iwasawa, *Surf. Sci.*, 1995, **343**, 1–16.
- 5 S. S. Fu and G. A. Somorjai, *Surf. Sci.*, 1992, **262**, 68–76.
- 6 H. -L Schmidt and E. Schmelz, *Chemie unserer Zeit*, 1980, **14**, 25–34.